Phonon propagation in liquid ^{4}He: the dependence on injected power and pressure

1989 J. Phys.: Condens. Matter 1 8629

(http://iopscience.iop.org/0953-8984/1/44/033)

J. Phys.: Condens. Matter **1** (1989) 8629–8648. Printed in the UK

Phonon propagation in liquid ^{4}He: the dependence on injected power and pressure

A F G Wyatt
Department of Physics, University of Exeter, Exeter EX4 4QL, UK

Received 30 June 1989

Abstract. The propagation of phonons in liquid ^{4}He is considered as a function of the number of phonons injected, the ambient pressure, the propagation distance and the ambient temperature. It is shown that there are four main groups of behaviour. The first and simplest is at high pressures, $P > 19$ bar, where apart from some phonon–roton scattering near the heater, the propagation is ballistic and independent of distance and temperature for $T < 0.3$ K. The second group is at low pressures and low injected phonon densities, where the behaviour is dominated by spontaneous decay and can be modelled satisfactorily. The third group is at low pressures and moderate injected phonon densities, where there is interaction within the beam between the high- and low-frequency phonons. The fourth group is at low pressures and high injected phonon densities, where interactions within the beam are so strong that there is frequency up-conversion to both medium and high phonon energies. The up-conversion process is suggested to be a combination of three- and four-phonon processes. At low pressures, the high-frequency phonons are attenuated by scattering with thermal phonons; however, the dependence of the attenuation on ambient temperature decreases as the injected phonon density increases, because the up-conversion reduces the effective distance for decay processes.

1. Introduction

Phonon propagation in liquid ^{4}He can be quite simple under the right conditions. If the liquid ^{4}He is cold, $T < 0.05$ K, and pressurised to $P > 19$ bar and few phonons are injected, then the propagation is ballistic without any scattering or decay processes. However, if any of these conditions are relaxed, then the situation can become complex. If the liquid ^{4}He bath temperature is raised, then there will be interactions with the thermal phonons [1]. If the pressure is lowered, then spontaneous phonon decay processes will occur [2–5]; and if the injected flux is too high, there will be scattering within the beam [6]. Rotons are injected with the phonons and these will scatter the phonons if the roton density is high enough [6].

In a previous paper [7]† we showed from velocity measurements that at low pressures and medium powers the injected phonons form two propagating groups (see figure 1). The faster group, which propagates at the ultrasonic velocity, is composed of low-energy phonons from the injection and spontaneous decay processes; and the slower group, moving at their group velocity, is composed of $\omega > \omega_c$ phonons. These high-energy

† The value of $2\Delta_{Al}$ printed in [7] is in error; it should be 385 μeV, which is equivalent to 4.47 K.

0953-8984/89/448629 + 20 $02.50

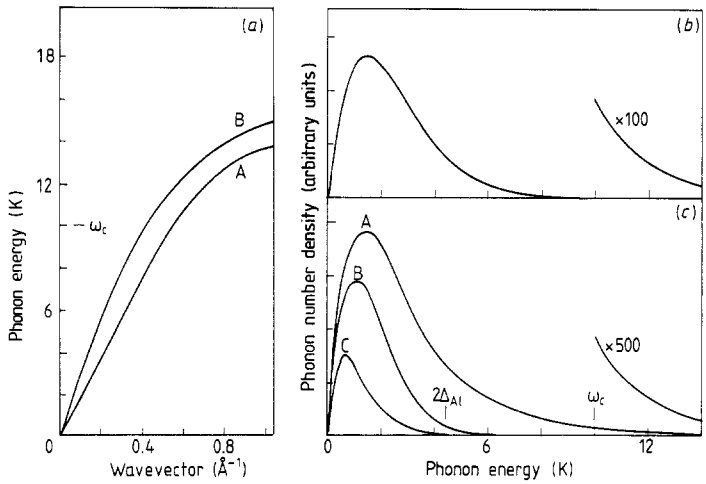

Figure 1. (*a*) Dispersion curve for phonons in liquid ^{4}He at 0 (curve A) and 25 (curve B) atm [8]. The minimum energy, ω_c, for macroscopic mean free paths is shown at 10 K. (*b*) The calculated number density as a function of energy. It is the sum of two Planck spectra, one at 0.9 K and the other at 1.85 K in the ratio of 1 to 5×10^{-3}, which represents a −20 dB (ref. 0.5 W mm^{-2}) input pulse [7]. (*c*) A schematic representation of the phonon number densities after propagation through the liquid ^{4}He, for low (curve A), medium (curve B) and high (curve C) injected input powers [7]. The positions of detector threshold energy, $2\Delta_{Al}$, and ω_c are shown. At low powers there are two distinct groups of phonons, one at low energies and the other with $\omega > 10$ K.

phonons are above the threshold, ω_c (10 K at 0 bar) [4], for spontaneous decay and so at low bath temperatures have long mean free paths, greater than 10 mm at least. As in [7], $\omega_c(P)$ is defined as the minimum phonon energy for macroscopic mean free paths at ambient pressure P.

In this paper we consider the size and shape of the detected signals and how they are affected by pressure, pulse power, bath temperature and distance. The important regions of the pressure and power space are shown in figure 2. Some of these regions can be understood better than others. At high pressures, interactions are not important, except to broaden the signal, and so the signal size increases approximately in proportion to the injected power for the whole power range. At low pressures and low powers the signal is dominated by spontaneous decay and a good understanding of the behaviour can be obtained. However, at low pressures and at medium and high powers the interactions are dominant and give a range of behaviours. Only a qualitative picture can be drawn in this case, but this is offset by the interesting effects that occur. The temperature and distance behaviour help to unravel the story.

One of the interesting features of the interactions is the up-conversion of phonons to energies above ω_c. In [7] we showed that interactions lead to the fast signal at the ultrasonic velocity. This requires interactions to create phonons with energies greater than the energy gap ($2\Delta_{Al}$) in the superconducting detector. The three-phonon scattering is sufficient for this. However, to elevate to $\omega > \omega_c$ there must be three- and higher-phonon scatterings to raise the energy to just below ω_c and then four-phonon scattering to take it above ω_c. At high powers this causes a considerable increase in the number of $\omega > \omega_c$ phonons.

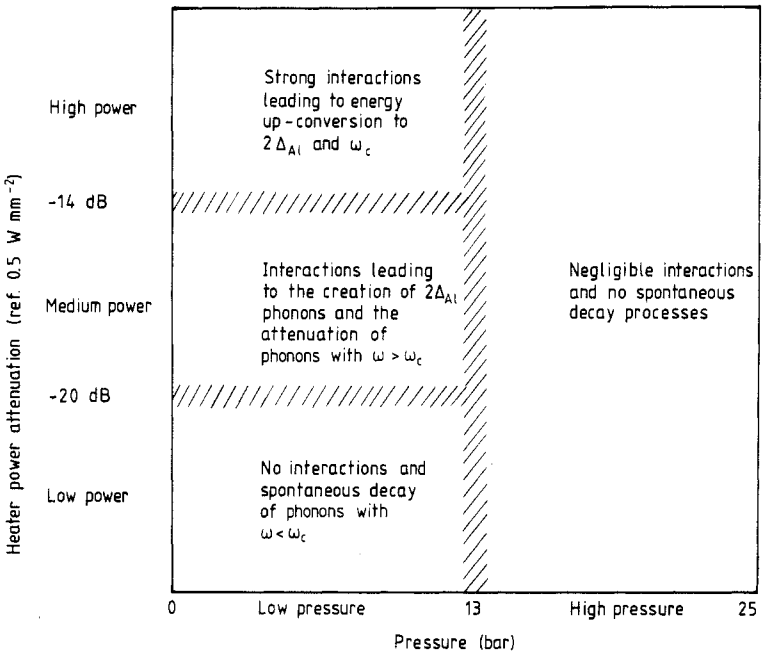

Figure 2. The different regions of the pressure–power space with the main characteristics of each region. The absolute high-pressure region is $P > 19$ bar, but for a detector with threshold energy $2\Delta_{Al} = 4.2$ K the critical pressure is 13 bar. The regions are referred to in the text as, for example, 'medium power and low pressure'.

Another interesting effect is the scattering of high-energy phonons, i.e. those with $\omega > \omega_c$, by low-energy phonons within the injected beam, through the four-phonon process. This can cause a decay of the $\omega > \omega_c$ phonons, even at the lowest ambient temperatures, when the injected energy is too high. The effect of this attenuation is to give a plateau in the growth of the $\omega > \omega_c$ phonon signal with heater power.

In § 2 the experimental arrangement is discussed, in § 3 is presented the results of the measured power and pressure dependences and in § 4 these results are discussed. In § 5 the effect of temperature at different powers and distances is presented and discussed, and conclusions are drawn in § 6.

2. Experimental arrangement

The experimental arrangement is the same as in [7]. A thin film heater faces a superconducting Al–I–Al tunnel junction both with dimensions 1×1 mm in a cell full of liquid ^4He. The separation between the heater and detector can be varied using a superconducting stepper motor.

The Al in the tunnel junction has an energy gap $2\Delta_{Al} = 4.5$ K (energies are expressed in kelvin throughout). The junction is biased at 365 μV and is able to detect signals over a wide dynamic range of more than 10^3. Even at the highest signal levels there is no over-injection and so it behaves as a linear detector. A superconducting tunnel junction detects phonons by pair breaking, so it is only sensitive to those phonons with $\omega > 2\Delta_{Al}$

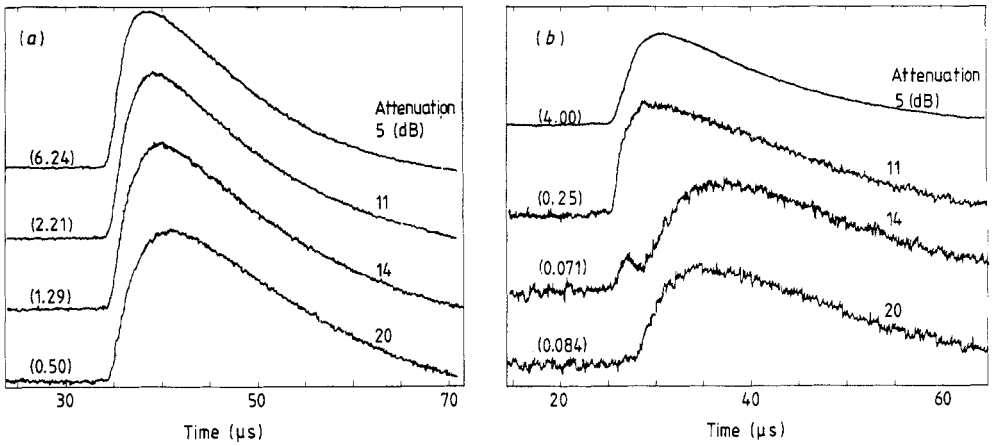

Figure 3. Typical pulse shapes at (*a*) 24 bar, 9.9 mm and (*b*) 6 bar, 7 mm respectively, at different heater powers referred to 0.5 W mm^{-2} and at $T = 0.1$ K. Time is measured from the start of the heater pulse. To obtain relative signal sizes the traces shown should be multiplied by the scale factors shown in brackets. The $2\Delta_{Al}$ and ω_c signals are resolved at 6 bar, 7 mm and 14 dB attenuation.

[9]. For phonons with $2\Delta_{Al} < \omega < 4\Delta_{Al}$ it is sensitive to phonon number rather than energy. At higher phonon energies the response may be enhanced by two mechanisms. A phonon with $\omega > 4\Delta_{Al}$ could break two pairs and also there may be an increased probability of transmission from the liquid ^{4}He to the Al film. The pressure dependence of the signal at low powers, in which the phonon energies are scanned by the pressure-dependent critical energy $\omega_c(P)$, indicates that any such-phonon energy dependence is negligible as there is no discontinuity at $\omega_c(P) = 4\Delta_{Al}$. The time constant of the detector is about 2 μs, which can be seen directly from the response to fast signals. In keeping with other metal film detectors, the superconducting tunnel junction is insensitive to rotons.

After amplification the signal is digitised by a Biomation 8100 transient recorder. Many repetitions of the signal are averaged to improve the signal-to-noise ratio. For the weakest signals over 10^5 repetitions are made.

The experimental cell is cooled by a simple dilution refrigerator and the temperature is measured with a 220 Ω Speer carbon resistor. The temperature values are not particularly accurate and if anything the quoted values are probably a little high, by about 10–20 mK at the lowest temperature. The heater pulse length is kept constant at 1 μs. Heater power densities are given in decibels (dB) and are referenced to 0.5 W mm^{-2}.

3. Measured power and pressure dependences

In figures 3(*a*) and (*b*) are shown typical detected signals at high and low pressures. At 24 bar the signal shapes broaden a little as the heater power decreases, but the main effect is the decrease in signal height. In contrast at 6 bar the signal shape changes qualitatively and also decreases more rapidly with heater power. At −14 dB heater power the detected signal shows two maxima and by −20 dB the faster pulse has

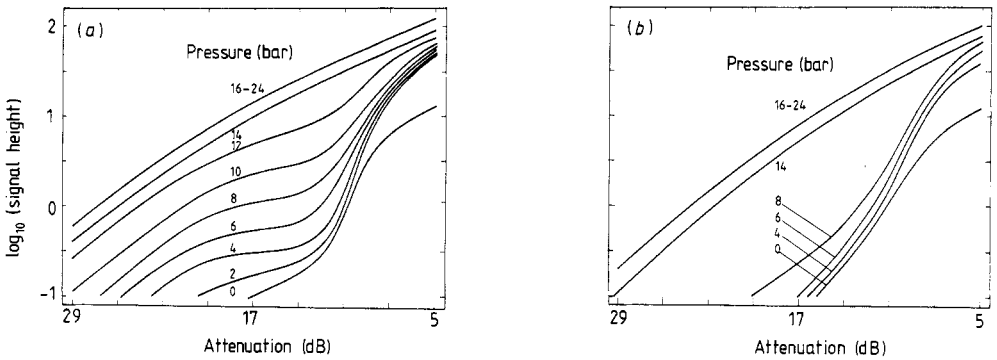

Figure 4. The logarithm of the signal as a function of heater power attenuation, referred to 0.5 W mm^{-2}, at different pressures and $T = 0.1$ K. The signals are (*a*) ω_c phonons and (*b*) $2\Delta_{Al}$ phonons (as defined in text below). The results for 16 to 24 bar are coincident within the random error. The measured points are omitted for the sake of clarity but they can be seen in figure 6, which comes from the same data.

disappeared. The signal heights that are used in this paper are measured from such traces at particular times.

To characterise the results we use two times. The fastest signal that is detectable by the superconducting tunnel junction is due to phonons with $\omega = 2\Delta_{Al}$. Phonons at this energy have essentially no dispersion and so give a peak signal about 1 μs (the pulse length) after the start of the signal, as over times less than τ_c the detector integrates the incident flux. At low powers the start of the signal is not always clearly defined, so we take the time of the start of high-power signals and define the strength of the $2\Delta_{Al}$ group of phonons as the signal height at 1 μs after this start time. As there is no dispersion a range of phonons with $\omega > 2\Delta_{Al}$ arrive at this time. This procedure means we take the peak height of the fast signal when it is resolved, as at -14 dB at 6 bar and 7 mm shown in figure 3(*b*).

For the ω_c group we take the signal 5 μs after the start of the slow pulse for a heater–detector distance of 2.3 mm. Although we measure the signal height at a particular time, we do not believe that this corresponds to a particular phonon energy. Phonons with $\omega > \omega_c$ have considerable dispersion, which gives a significant broadening of the pulse with distance. However, there is phonon–roton scattering near the heater [6], which broadens the pulse at all distances as discussed in § 4 and this, together with the detector time constant, means that a range of high-energy phonons contribute at the ω_c time. It is for these reasons that the ω_c signal is best measured at 5 μs after the start of the slow signal. We shall see in § 4 that this signal is dominated by phonons just above $\omega_c(P)$.

In figures 4(*a*) and (*b*) we show the signal height as a function of the input power on log–log scales for pressures between 0 and 24 bar. The measured points are omitted for the sake of clarity but they are shown later in figures 6(*a*) and (*b*), which come from the same data. We have chosen a small distance, 2.3 mm, between the heater and detector so that signals can be measured down to low powers. In the range it can be measured, the pattern is the same at larger distances.

In figure 4(*b*) the data between 8 and 14 bar have been omitted from the diagram because the two groups of phonons overlap at these pressures. This happens because $\omega_c(P)$ decreases with pressure and the ω_c phonons arrive at the same time as the $2\Delta_{Al}$

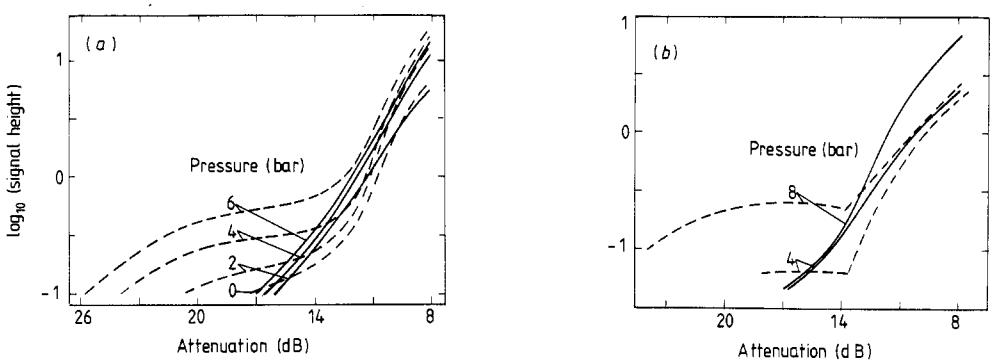

Figure 5. The logarithm of the signal as a function of heater power attenuation, referred to 0.5 W mm^{-2}, at different low pressures and $T = 0.1$ K. The figures are for heater–detector distances of (*a*) 2.3 and (*b*) 4.6. The full curves are for $2\Delta_{Al}$ signals and the broken curves are for ω_c signals.

phonons. At low powers the $2\Delta_{Al}$ signal is smaller than the ω_c signal and so it cannot be extracted from the combined signal.

The results shown in figures 4(*a*) and (*b*) extend over a wide range of signal sizes; three orders of magnitude are shown. For pressures between 16 and 24 bar the signal does not depend on pressure, and it increases approximately linearly with power in both figures. This is because at high pressures we are dealing with the same non-interacting group of phonons in both figures. The small difference between the two curves reflects the change in shape of the high-pressure signal with power. The curve in figure 4(*b*) is sensitive to the leading edge of the signal pulse and this rises faster with power than the ω_c signal shown in figure 4(*a*).

At low pressures the behaviour is quite different from that at high pressures; moreover the signals at the two arrival times behave differently with power. The ω_c signal shows a plateau at -17 dB where the signal is independent of power. For powers between -11 and -8 dB the signal rises very rapidly, while at low powers, less than -20 dB, the signal increases approximately linearly with power. In contrast the $2\Delta_{Al}$ signal (figure 4(*b*)) is small and difficult to detect below about -17 dB. At higher powers it shows a rapid increase with power, which is similar to the ω_c signal. The major difference between the two figures is therefore at low powers and low pressures.

To emphasise this last point we show in figure 5(*a*) the low-pressure data of figure 4(*a*) and (*b*) together, and in figure 5(*b*) we show similar data for 4.6 mm heater–detector separation. At this distance the plateau region for the ω_c signal is more marked.

In figure 6(*a*) are shown the same ω_c data as in figure 4(*a*) but pressure is now the ordinate. For powers less than -17 dB the logarithm of the signal rises approximately linearly with pressure up to 13 bar. Similarly the $2\Delta_{Al}$ data in figure 6(*b*) are the same as in figure 4(*b*). For pressures $P < 8$ bar and low powers less than -14 dB, the signal is independent of pressure, which contrasts sharply with the behaviour of the ω_c phonon signal. The rise in signal between 8 and 14 bar is due to the ω_c signal overlapping the $2\Delta_{Al}$ signal, so the rise has the same origin as the linear increase in figure 6(*a*). It is therefore only at pressures $P < 8$ bar where the data relate clearly to interacting phonons, although interactions are still possible up to $P \sim 19$ bar where ω_c becomes zero [10, 11].

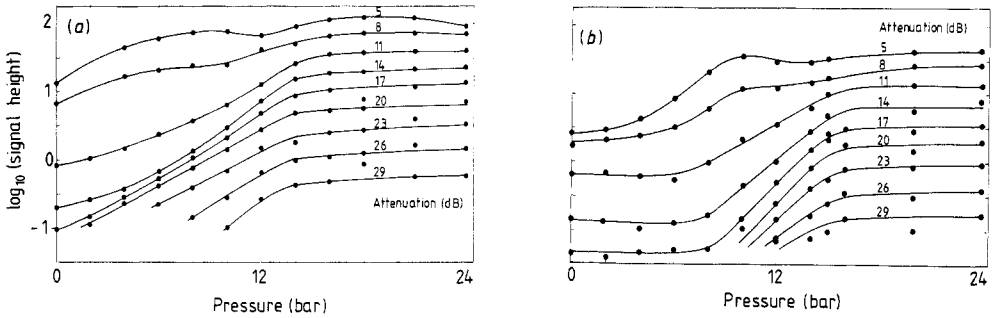

Figure 6. The data in figure 4 shown as a function of pressure for different heater power at $T = 0.1$ K. (*a*) ω_c phonons, and (*b*) $2\Delta_{Al}$ phonons. Note the large difference in behaviour at low pressures at both low and high powers.

4. Discussion of power and pressure dependences

We now discuss the data in four sections: (i) at high pressures, $P > 16$ bar, where $\omega_c < 2$ K [4] and interaction between the phonons is negligible at all powers; (ii) at low pressures and low powers, where the density of phonons is too low for interactions to be important and spontaneous decay processes determine the behaviour; (iii) at low pressures and medium powers, where the $\omega > \omega_c$ phonons interact with the low-energy phonons within the beam; and (iv) at low pressures and high powers, where we expect to find large effects due to interactions.

4.1. High pressures and all powers (negligible phonon–phonon scattering)

The basic behaviour at high pressures can be stated quite simply. Phonons that are injected into the liquid ^{4}He travel to the detector essentially ballistically. Increasing the pulse power to the heater injects more phonons without changing the spectral distribution. So the fraction of phonons above $2\Delta_{Al} = 4.5$ K remains the same and the signal increases linearly with power. For the plot used in figure 4 this picture would give a straight line with unit gradient and be pressure-independent. The measured results for pressure $P > 16$ bar are indeed coincident and show a gradient slightly greater than 1 at low powers and slightly less than 1 at high powers.

Underlying this concisely stated picture are a number of other results and assumptions, which we now examine. A hot solid injects phonons into liquid ^{4}He both elastically and inelastically. These two phonon channels are seen with cleaved surfaces of single crystals [12]. The ω conserving transmission gives a cone of phonons perpendicular to the surface and hence a peak in the angular distribution. For the rough surface of a heater these peak phonons are injected over a broad angular range. A phonon in the solid can also create two or three phonons in the liquid ^{4}He, and these phonons have a low energy and are injected in all directions into the liquid [12, 13]. These so-called background phonons carry, by far, most of the energy and we can neglect the peak phonons at high pressures. The effective temperature of the background phonons has been estimated in two different ways and it is about 0.9 K [14, 15] for powers between -20 and -14 dB.

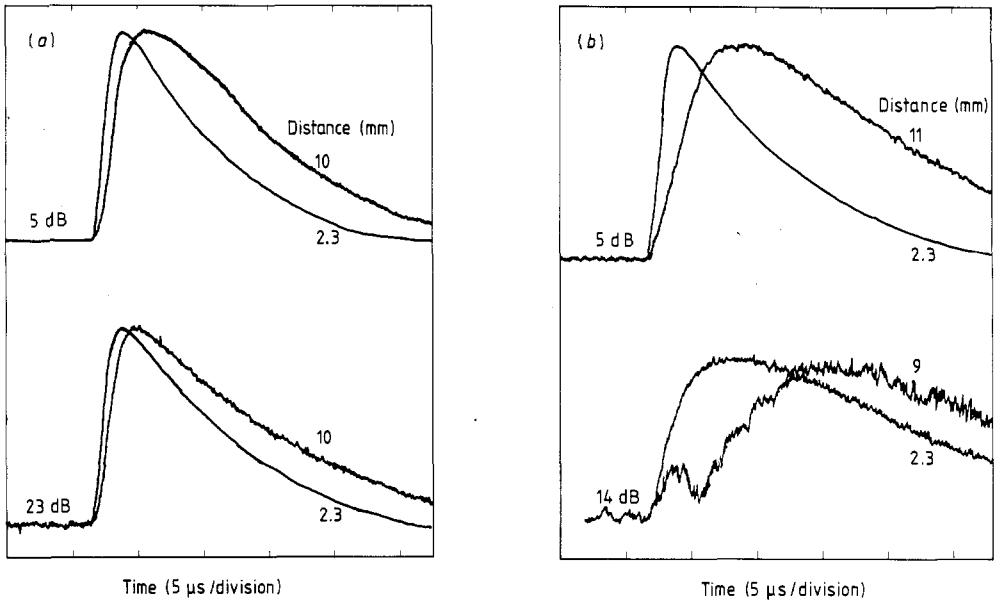

Figure 7. Typical signals at (*a*) 21 bar and (*b*) 6 bar showing the effect of distance at 0.1 K. Each pair of signals at the same power and pressure have been normalised and shifted along the time axis so that the start of the signals are coincident. The effect of dispersion, which can be seen as an increase in the width of the signal with distance, is greater at low pressures.

We know from quantum evaporation experiments that a heater injects rotons as well as phonons into the liquid He [16]. Metal film detectors are insensitive to rotons, probably because their reflection coefficient is essentially unity. So the superconducting tunnel junction signal only indicates the phonon flux. Rotons are produced even at the lowest powers, but the relative efficiency of producing phonons and rotons is not known, so we shall assume that the ratio is not too dependent on power. At first sight this may seem strange, as it might be expected that as the heater temperature increases it is easier to produce the high-energy rotons. However, the phonon transmission also rises with heater temperature, as is well known from the Kapitza effect [17].

Not only is the injected energy shared between phonons and rotons, but the rotons can scatter the phonons [6]. The scattering varies with wavevector (q) as q^4 [1], so the high-energy phonons are scattered more than the low-energy ones. In fact the evidence is that phonons with low energy, say $\omega < 3$ K, can propagate through the rotons at powers less than -20 dB [15], while phonons with $\omega > 10$ K are strongly scattered [6]. The first phonons produced in the heater pulse can propagate freely away from the heater; however after the pulse has been on for about 0.3 μs the roton density prevents any more of the $\omega > 10$ K phonons escaping from the region near the heater.

As the aluminium tunnel junction detector is sensitive to phonons with $\omega > 4.5$ K, we are dealing with a range of fairly high-energy phonons. We should therefore expect that some of these phonons travel ballistically between heater and detector while others have to diffuse through the roton cloud near the heater before escaping into essentially roton-free liquid ^{4}He. The pulse shape of the detected signal suports this idea. In figure 7(*a*) are shown received pulse shapes for 21 bar pressure, at high and low power and two distances. The pulse at 2.3 mm has a fast leading edge at all powers but a width at half

height of about 10 μs. This suggests a strong ballistic signal followed by phonons that escape from the roton cloud.

Other pulse stretching possibilities are: (i) finite size of the heater and detector—however this only stretches the pulse by about 0.5 μs; (ii) dispersion, but this will only broaden the pulse by a few microseconds as there are relatively few phonons with high energies that move slowly. For example for a heater–detector separation of 2.3 mm the difference in ballistic propagation times for ultrasonic and ω_c phonons is 5.5 μs. However the number of phonons with $\omega > 11$ K in a Planck distribution for a temperature of 0.9 K is about 3×10^{-3} of the number with $\omega > 4.5$ K, and so the phonons with $\omega > 11$ K do not contribute significantly to the detected pulse.

So at 2.3 mm we conclude that the signal shape is dominated by phonon–roton scattering. However, for longer distances the signal is broader, as can be seen in figure 7(*a*). This is most likely to be due to dispersion.

The faster than linear rise of the signal with power, at low powers and high pressures, could possibly be due to the phonon channel increasing somewhat faster than the roton channel as the temperature of the heater increased. The slower than linear rise at high powers is possibly due to the roton trapping becoming more effective with the higher density of rotons.

4.2. Low pressures and low powers (spontaneous decay and no interactions)

The propagation of phonons in liquid ^{4}He at low pressures is dominated by phonon decay processes [4, 5]. At low powers the density of phonons is small, so that mutual scattering can be ignored. This applies for powers less than −17 dB. Initially we neglect any interactions with thermal phonons.

Under these conditions the injected phonon spectrum changes in the bulk liquid by phonon decay, in which a phonon spontaneously decays into two or more phonons with conservation of energy and momentum. This process is allowed by the initial upward curvature of the dispersion curve [18]. This upward curvature diminishes with pressure and is zero at $P = 19$ bar [12]. At zero pressure, phonons with energy $\omega < 10$ K can decay this way. Although the mean free path for decay has not been measured it is certainly much less than 10^{-3} m for the higher-energy phonons. Theoretical models of the three-phonon decay process [19, 20] indicate that the mean free path varies as ω^{-5} and can be as small as 10^{-8} m for ω_c at 0 bar. As the pressure is increased the maximum energy for phonon decay, $\omega_c(P)$, decreases approximately linearly. At 6 bar, $\omega_c = 7.6$ K [4]. Phonons with energy $\omega > \omega_c$ cannot spontaneously decay, so these phonons have macroscopic mean free paths if there are no thermal phonons from which to scatter.

An injected spectrum of phonons changes very rapidly as it propagates. Phonons with $\omega < \omega_c$ decay in a cascade until they reach low enough energies for there to be no further decays in a distance of order of the heater–detector separation. Using the theoretical value of the frequency-dependent mean free path, we estimate that phonons decay to an energy $\omega \sim 0.7$ K. The spectrum of phonons arriving at the detector then has a gap from an energy of a few kelvin up to ω_c (see figure 1(*c*)). As the superconducting tunnel junction is only sensitive to phonons with $\omega > 4.5$ K, only the phonons with $\omega > \omega_c(P)$ are detected for $P < 13$ bar.

The predominant contribution of high-energy phonons to the signal at low pressures can be seen in the large dispersion of the pulse shapes with distance. Comparing the

signals in figure 7(*b*) with those in figure 7(*a*), the much larger dispersion with distance can be seen at 6 bar compared to 21 bar.

It is expected that these ω_c signals will be very pressure-dependent due to ω_c changing with pressure. We first estimate the pressure dependence by assuming that the high-energy part of the injected spectrum varies approximately as $\exp(-\omega/T_e)$ where T_e is the characteristic temperature of the spectrum, and that the cut-off energy varies approximately as $\omega_c = 10(1 - P/19)$ K where P is the pressure in bars [4]. The number of phonons (S) with $\omega = \omega_c$ varies as $S = S_0 \exp(-\omega_c/T_e)$, so that [5]

$$\log_{10}\left(\frac{S}{S_0}\right) = \frac{4.34}{T_e}\left(\frac{p}{19} - 1\right). \tag{1}$$

We immediately see the origin of the nearly straight lines at low powers and low pressures in figure 6(*a*).

To improve on this estimate we must consider the injected spectrum in more detail. As mentioned earlier, the heater injects both peak (energy conserving) and background (energy down-converted) phonons. The peak phonons reflect the temperature of the heater (T_h) which is for example 1.85 K at −20 dB heater power [21], while the background phonons have an effective temperature of $T_b = 0.9$ K independent of power [12, 13]. Although the total number of background phonons is much higher than that of peak phonons, the ratio becomes less at high frequencies because $\exp(-\omega/T_b) \ll \exp(-\omega/T_h)$.

Following [7], we take the intensity of phonons with energy $\omega = 10$ K to be equal for peak and background channels at a heater power of −20 dB. For energies $\omega > 10$ K the spectrum is increasingly dominated by the peak channel as ω increases because of its higher characteristic temperature, while for $\omega < 10$ K the spectrum reflects more the background channel as ω decreases. This means that as the pressure is increased and ω_c decreases, the signal becomes dominated by the constant temperature of the background channel.

When the pressure is such that $\omega_c = 4.5$ K, the detector threshold, any further increase in pressure has no effect on the detected signal. This gives rise to the pressure-independent signals above $P = 14$ bar, which can be clearly seen in figure 6(*a*). The pressure of the knee in $\log_{10} S$ against pressure can be estimated from the energy gap in the superconducting aluminium measured from the tunnelling I–V characteristic, and the measured values of $\omega_c(P)$ [4]. This estimate gives $P \sim 13$ bar, which is in good agreement with the results in figure 6(*a*).

The phonon spectrum injected by −20 dB heater pulse is given by [7]

$$N(\omega) = A\omega^2(e^{-\omega/0.9} + 5 \times 10^{-3}\, e^{-\omega/1.85}) \tag{2}$$

where A is unknown and is treated as the adjustable constant. The number of phonons at $\omega_c(P)$ can then be found using the measured values of $\omega_c(P)$. In figure 8 we show the results of calculating $\log N(\omega_c)$ as a function of pressure. The full circles show the measured ω_c signal for −20 dB and 2.3 mm heater–detector distance. The good agreement indicates that the ω_c signal is due to phonons around $\omega_c(P)$.

4.3. Low pressures and medium powers (spontaneous decay and interactions among the injected phonons)

At low pressures and low powers we only detect the phonons with $\omega > \omega_c$. This signal rises approximately linearly with heater power due to the injection of background

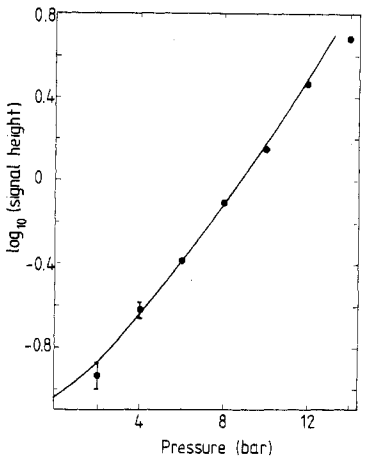

Figure 8. The logarithm of the height of the ω_c phonon signal as a function of pressure at $T = 0.1$ K. The points are measured at -20 dB, reference 0.5 W mm^{-2}, heater power and 2.3 mm heater–detector separation. The curve is calculated as described in the text.

phonons, which increase proportionately with power. However, for powers greater than about -20 dB, the signal stops rising so quickly and a plateau forms by -17 dB and ends at -14 dB, where the signal increases rapidly. This can be seen in figure 4(*a*). The width of the plateau increases with the heater–detector separation (figures 5(*a*) and (*b*)).

In the plateau region the logarithm of the signal still rises linearly with pressure as it did at low powers, which shows that we are still dealing with $\omega > \omega_c$ phonons. However, the existence of the plateau indicates that we are detecting a smaller fraction of the injected phonons with $\omega > \omega_c$ as power increases.

We suggest that the number of high-frequency phonons ($\omega > \omega_c$) is reduced by scattering within the beam. As we have noted earlier, only a small fraction of the energy is injected as high-frequency phonons, most of the energy being emitted at low frequencies and being further down-converted by three-phonon decays. At low powers these two groups of phonons are independent, but as the power is increased the relatively weak four-phonon interaction becomes significant due to the higher frequency of encounter between high- and low-energy phonons.

In a four-phonon scattering process a high- and low-energy phonon are annihilated and a similar pair of phonons are created [1]. The energies are slightly changed as is the direction of the high-energy phonon. This process by itself cannot change the detected signal, as the high-energy phonon still has $\omega > 2\Delta_{Al}$. However, many such scatterings can reduce the energy of the high-energy phonon to below ω_c and then the relatively strong spontaneous phonon decay processes can quickly reduce the energy to less than $2\Delta_{Al}$ [22].

Evidence from the temperature dependence of the signals at different powers supports this picture. As the bath temperature is raised the signal measured at -20 dB decreases more than the one at -14 dB. If the signal at -14 dB is already reduced by scattering from injected phonons, then the thermal phonon density has to be increased until it is comparable with the injected phonon density for it to have any significant effect. At -20 dB, the number of injected low-energy phonons is not causing much attenuation and so thermal phonons have an effect at lower temperatures.

The plateau extends to lower powers as the propagation distance is increased. This follows from the model as there is more time for four-phonon scattering and hence more chance of decays below ω_c.

As the pressure is increased the plateau fades away at pressures between 12 and 14 bar, which shows that the decrease in signal at lower pressures is controlled by the spontaneous phonon decay process, which ceases to be effective above 13 bar where $\omega_c = 2\Delta_{Al}$. However, this phonon decay process alone cannot affect the signal as the signal is solely due to phonons with $\omega > \omega_c(P)$, as indicated by the pressure dependence.

4.4. Low pressures and high powers (strong interactions and up-conversions)

In the previous sections we saw that a model based on phonon decay processes explained the low-pressure data up to about -14 dB, for the $\omega > \omega_c$ phonons. However, for powers greater than -17 dB, another signal besides the one for $\omega > \omega_c$ phonon begins to appear. This can be seen in figure 3(*b*) for -14 dB and 6 bar. This is a fast signal, which travels at the ultrasonic velocity and shows no dispersion. At low pressures, $P \sim 8$ bar, it can be seen separately from the slower phonons with $\omega > \omega_c$. This fast signal grows very rapidly with power, as can be seen in figure 4(*b*); however it is pressure-independent, at least up to 8 bar, as can be seen in figure 6(*b*).

This fast signal, which only appears at high powers, is ascribed to interactions among the injected phonons, which push the high ω tail of the spectrum of the low-energy phonons above the detector energy threshold, $2\Delta_{Al}$. As interactions require a high density of phonons, it only occurs at high powers.

We picture the following sequence. Phonons injected into the ^{4}He have mainly low energies and those with $\omega > 1$ K rapidly decay to low energies quite near to the heater. The density builds up and they interact through the three-phonon process, which produces up-conversion [23] as well as decay. The spectrum broadens and the tail extends to higher frequencies by an increasing amount as the power is increased. The exact position of $\omega_c(P)$ is not important providing $\omega_c(P) > 2\Delta_{Al}$; also the strength of the three-phonon scattering is immaterial providing it is strong enough for frequent scattering on the timescale of the pulse. Hence we see that the $2\Delta_{Al}$ signal is pressure-independent for $P < 8$ bar.

The growth of signal with power can be very strong; the signal from the ω_c phonons rises by a factor of 20 for a doubling of the heater power. Apart from at 0 bar, the signals rise to within a factor of 3 of the high-pressure signal at -5 dB. The $2\Delta_{Al}$ phonon signal starts to rise at a slightly lower power, -17 dB compared to -12 dB for the ω_c signal (see figures 4(*a*) and (*b*)) and the rise is not quite as rapid. Signals at -5 dB are similar in size to the high-pressure value, which indicates that the number of phonons with $\omega > 2\Delta_{Al}$ is approaching that injected.

The signals at the two arrival times increase rapidly with power due to the rate of interactions between the phonons increasing with phonon density. It is suggested that phonons are up-converted to $\omega > \omega_c$ in two stages. First, phonon energies are up-converted by the inverse of the spontaneous decay processes. This can elevate phonons up to but not beyond ω_c. At this energy the phonon can undergo a four-phonon scattering, which can take it above ω_c. As the four-phonon process is weak, this final stage in the up-conversion has a low probability; however it also means, by reciprocity, that the $\omega > \omega_c$ phonon is relatively stable.

Some insight into the power dependence of the interaction signal can be obtained from the following simple example. Among the group of low-energy phonons there will be some small fraction with $\omega = 2$ K. At a low heater power there will be negligibly few phonons with $\omega > 4$ K and so there is no signal from this group. As the heater energy is increased the density (n_2) of $\omega = 2$ K phonons increases and they begin to collide. The

three-phonon process enables two 2 K phonons to annihilate and create one phonon with $\omega = 4$ K. This phonon will after a short time spontaneously decay into two phonons, which most probably will be equal in energy. As the decay time τ is short ($\tau = \lambda/c \sim 10^{-8}$ s), a dynamic equilibrium occurs with a finite density (n_4) of $\omega = 4$ K phonons. As the number of interactions of 2 K phonons increases as the square of the density, we have

$$An_2^2 = n_4/\tau \tag{3}$$

where A is a constant determined by the strength of the three-phonon process.

We might expect n_2 to increase approximately linearly with the heater power, so we see from equation (3) that the detected signal from the 4 K phonons increases quadratically with power. Despite the crudeness of the model this dependence is seen for the fast signal; see figure 4(*b*) for powers less than −11 dB. At higher powers the power dependence increases more quickly as n_2 increases faster than linearly with power. However, at even higher powers this picture breaks down and the group of low-energy phonons becomes so strongly interacting that they are essentially thermalised, although not isotropically distributed. The characteristic temperature cannot be as high as that for injected background phonons from which the interacting phonons mainly originate. So the number of phonons with $\omega > 2\Delta_{Al}$ at low pressures cannot exceed that at high pressures, and this means that the increase of the interacting phonon signal must slow down and finally increase approximately linearly with power.

The increase in the ω_c signal is faster with power than the $2\Delta_{Al}$ signal. In the process that we suggest for the creation of $\omega > \omega_c$ phonons, phonon scattering has first to create phonons near to ω_c. In fact three-phonon processes can only take the energy to $\omega =$ 8.5 K at 0 bar, but processes where n small phonons, annihilate to create one large phonon can take the energy to ω_c. Returning to our simple model, the probability of n phonons scattering simultaneously is small but increases as the nth power of the phonon number density. Another route, whereby 2 K phonons create 4 K which then create 8 K phonons by three-phonon scattering, increases as the four power. While not taking the details of these models very seriously, they do show that the production of high-energy phonons should increase rapidly with power.

5. Temperature dependences

5.1. High pressures

At high pressures the signals are little affected by the liquid ^4He temperature, whether the heater power is high or low. This is in sharp contrast to the behaviour at low pressures, where there can be strong temperature dependences. This clearly indicates that scattering by thermal phonons is only effective in reducing the signal if three-phonon scattering is allowed. The relatively weak four-phonon scattering that is possible at high pressure is not effective in down-converting the energy of a significant number of phonons.

5.2. Low pressures

At low pressures, $P < 8$ bar, the effect of temperature depends on the power and the heater–detector distance. At high powers and short distances the temperature

Table 1. The change in signal due to a change in the ambient temperature from 0.1 to 0.3 K at 6 bar pressure. Only at −14 dB could the $2\Delta_{Al}$ and the ω_c signals be resolved and then not at 2.3 mm. The leading edge of the −5 dB signal showed less change with temperature than the ω_c signal, e.g. about a factor of 4 decrease at 11.0 mm.

	Heater power (ref. 0.5 W mm^{-2})			
Heater–detector separation	−5 dB	−14 dB		−20 dB
	ω_c phonons	$2\Delta_{Al}$ phonons	ω_c phonons	ω_c phonons
2.3 mm	4% increase	40 (±30)% increase	10% decrease	2× decrease
7.0 mm	4× decrease	no change	4× decrease	10× decrease
11.0 mm	13× decrease	2× decrease	7× decrease	no data

dependence is negligible, while at long distances the dependence is strong for all powers. At medium powers and distances there are signals from the interacting phonons and the $\omega > \omega_c$ phonons that have very different temperature dependences. The interacting phonons are hardly affected while the $\omega > \omega_c$ ones are much reduced. Representative signals are shown in figures 9, 10 and 11 and the basic behaviours are summarised in table 1.

The effect of increasing the bath temperature is mainly to attenuate the phonons with $\omega > \omega_c$. This is through four-phonon scattering with the thermal phonons until $\omega < \omega_c$ and then spontaneous decay to low energies [22]. An increase in the number of thermal phonons has little effect on the phonons with $\omega \sim 2\Delta_{Al}$. This can be seen in figure 12.

The reason why the effect of temperature depends on the injected power and heater–detector distance is as follows. At high excitation densities the phonons are strongly interacting within the pulse and there is a dynamic equilibrium that maintains the number of $\omega > \omega_c$ phonons. Extra low-energy phonons have little effect on this system. However, as the distance from the heat is increased, the excitation density falls due to geometric spreading and the interactions become less frequent. The decay processes will then outweigh the up-conversion at some distance from the heater. So the effect of interactions is to reduce the effective distance over which the thermally induced decay can operate. We should therefore expect that the temperature dependence will be less for higher powers at a given heater–detector separation, and this is generally found in the measurements (see table 1).

We now consider in turn the temperature and distance dependences at three representative powers, −5, −14 and −20 dB.

5.2.1. High powers at low pressures. At high powers there is a high density of excitations just in front of the heater. The interactions between the phonons will therefore be strong and this will give a large number of phonons above $2\Delta_{Al}$. Close to the heater we expect the up-conversion to be so strong that phonons cover the whole spectrum, even above ω_c, which is 7.6 K for 6 bar pressure. We shall see that the creation of phonons with

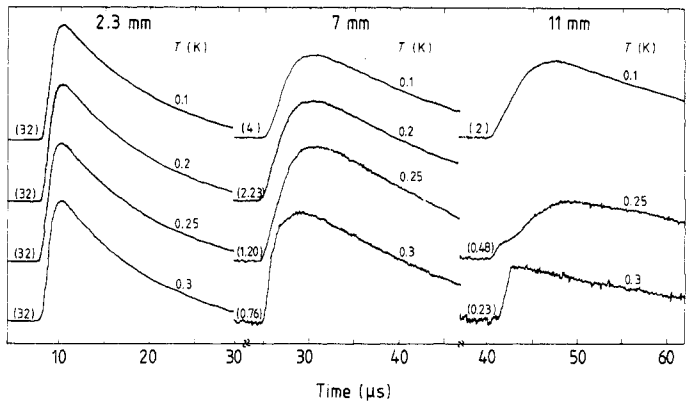

Figure 9. Typical pulse shapes at 5 dB attenuation (reference 0.5 W mm^{-2}) and 6 bar, showing the effect of ambient temperature at different distances. To obtain relative signal sizes the traces shown should be multiplied by the scale factors shown in brackets. It can be seen that the temperature dependence increases with distance and the pulse shape also changes with distance.

$\omega > \omega_c$, so that the total number exceeds the number injected, is necessary to explain the temperature and distance dependences.

For short heater–detector distances (2.3 mm) we see in figure 9(*a*) a large signal with a fast leading edge. It is only weakly temperature-dependent, as the thermal phonons do not much increase the density of low-energy phonons, which are already there from the injection pulse. In fact the signal slightly increases with temperature, which we attribute to an increase in the rate of up-scattering.

As the distance from the heater is increased to 7 mm, the density of phonons is reduced by geometric spreading and so the interaction rate reduces. Although scattering keeps a population of phonons above $2\Delta_{Al} = 4.5$ K, we see that there is virtually no up-conversion to $\omega > \omega_c$, as this signal is temperature-dependent. These phonons will not decay at low bath temperatures; however, as the bath temperature is increased, the phonons with $\omega > \omega_c$ are attenuated while those with $2\Delta < \omega < \omega_c$ are hardly affected. The increasing proportion of the faster low-frequency phonons with temperature can be seen in the speeding-up of the leading edge of the signal with temperature in figure 9(*b*). The attenuation of the $\omega > \omega_c$ phonons starts a few millimetres away from the heater, where the interactions, scattering to $\omega > \omega_c$, die away. This means that the temperature attenuation factor is less than at low powers, where the only phonons with $\omega > \omega_c$ are those injected and these have a longer distance in which to decay.

At the largest distance, 11 mm, we get mostly $\omega > \omega_c$ phonons and fewer $\omega > 2\Delta_{Al}$ phonons from interactions because of the further drop in phonon density. The signal is very temperature-dependent, as can be seen in figure 9(*c*). At $T = 0.25$ K the signal shows two contributions, the faster one from $\omega \sim 2\Delta_{Al}$ phonons and the slower one from $\omega > \omega_c$ phonons. The resolution of the two contributions arises from the preferential attenuation of the phonons just above ω_c, as these are most likely to scatter over the ω_c edge [23]. By $T = 0.3$ K the only phonons that are left are those with $\omega \sim 2\Delta_{Al}$ and they are spread out in time, probably by scattering. This may also account for the slightly later take-off than at lower temperatures, an effect that can be seen in figure 9(*c*).

5.2.2. Medium powers at low pressures. At −14 dB there is a lower density of excitations, which in turn means fewer interactions. However, they are not negligible and phonons

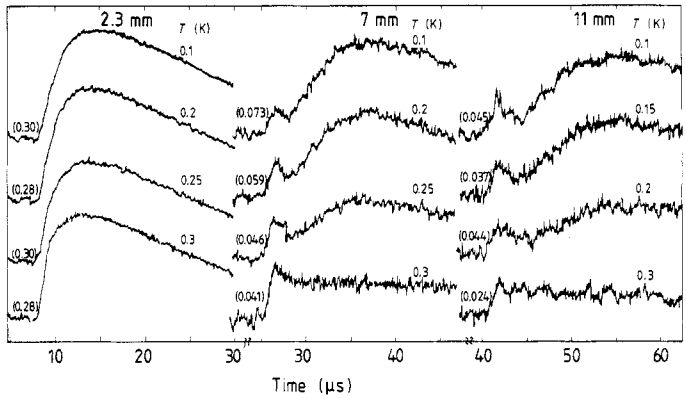

Figure 10. Typical pulse shapes at 14 dB attenuation (reference 0.5 W mm^{-2}) and 6 bar, showing the effect of ambient temperature at different distances. To obtain relative signal sizes the traces shown should be multiplied by the scale factors shown in brackets. The effect of temperature can be seen to be greater for the ω_c phonons than for the faster $2\Delta_{Al}$ phonons.

with $\omega > 2\Delta_{Al}$ are produced. Instead of increasing the number of $\omega > \omega_c$ phonons, as happens at higher powers, the interactions at -14 dB decrease the number of these phonons. As discussed in § 4.3 this comes from scattering of the $\omega > \omega_c$ phonons by the injected low ω phonons. Temperature has little effect until the scattering from thermal phonons reaches a comparable rate.

The effect of fewer interactions can be seen in the difference in pulse shapes at -5 and -14 dB at the closest distance and lowest temperature, in figures 9 and 10. The more rounded pulse shape at -14 dB is due to relatively fewer $\omega > 2\Delta_{Al}$ phonons compared to those with $\omega > \omega_c$. The $\omega > 2\Delta_{Al}$ phonons give the sharp rising edge at -5 db. As the bath temperature is raised, the leading edge at -14 dB becomes slightly stronger due to the increase in $\omega > 2\Delta_{Al}$ phonons by up-conversion.

As the distance is increased to 7 mm the signal shape changes considerably. In figure 10 it can be seen that the fast $\omega > 2\Delta_{Al}$ peak is clearly separated from the $\omega > \omega_c$ phonon signal. Besides dispersion the change from 2.3 mm is due to a drop in $\omega > 2\Delta_{Al}$ signal caused by the reduced rate of interactions as the phonon density decreases. The $\omega > \omega_c$ phonons, at low temperatures, are only reduced by geometric spreading and so they become relatively stronger.

At 7 mm the $\omega > \omega_c$ phonons are not scattered by the injected low ω phonons, as geometric spreading has reduced both phonon densities. So there is a temperature dependence due to scattering from the thermal phonons. However, this only effectively occurs over the flight path after the scattering from injected low ω phonons has stopped. The temperature dependence is therefore less than at lower powers at the same distance.

Just as there is a similarity between signals at -14 dB, 2.3 mm with those at -5 dB, 7 mm, there is one between -14 dB, 7 mm and -5 dB, 11 mm. To some extent the effect of lower powers can be offset by shorter distances. However, this is not generally true, and the effect of increased distance on the interacting phonons is not as strong as geometrical spreading would suggest.

At 11 mm the two contributions can be seen with the $\omega > \omega_c$ signal more attenuated than the $\omega > 2\Delta_{Al}$ one. The time difference between them has increased as expected from the different group velocities. The fast $\omega > 2\Delta_{Al}$ signal is possibly from previous

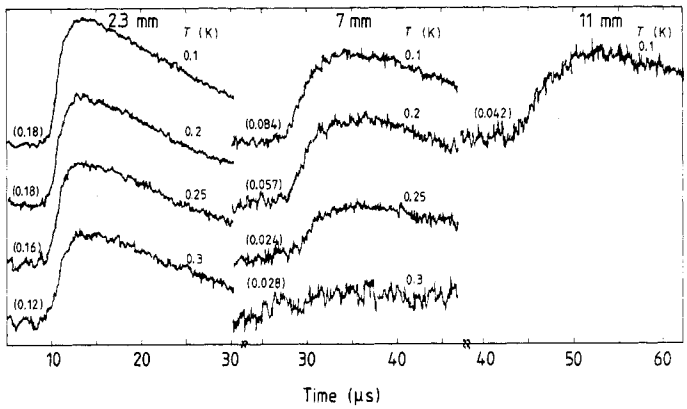

Figure 11. Typical pulse shapes at 20 dB attenuation (reference 0.5 W mm^{-2}) and 6 bar, showing the effect of ambient temperature at different distances. To obtain relative signal sizes the traces shown should be multiplied by the scale factors shown in brackets. The fast $2\Delta_{Al}$ phonon signal is absent at this low power. The high-energy phonons are strongly attenuated by thermal phonons and the effect is greater at larger distances.

up-conversion or from the decay products of spontaneous decay. In either case, the fast velocity indicates that we must be looking at the phonons that have escaped decay rather than ones formed by interactions near the heater. There remains the possibility that this very small signal may be due to phonons with $\omega < 2\Delta_{Al}$ being detected by a slightly non-ideal tunnel junction.

The $\omega > \omega_c$ signal decreases with bath temperature faster at 11 mm than at 7 mm. This is to be expected as the greater path difference gives more opportunity for decay. However, the effect of temperature at -14 dB is less than for -5 dB pulses at the same distance. At first sight this is a surprise because the shortening of the decay path by interactions near the heater should be greater at the higher power. The effect of temperature is ascribed to a difference in the spectra of phonons with $\omega > \omega_c$. At -5 dB most of the phonons with $\omega > \omega_c$ are near ω_c as they have come from a final four-phonon up-scattering process after up-conversion by three-phonon scattering. However, at -14 dB many of the phonons with $\omega > \omega_c$ are from the injection process, so there is a broader distribution. This picture is supported by the more dispersed signals at -14 dB, 7 mm and 11 mm, compared to those at -5 dB at the same distances (see figures 9 and 10). So the effect of four-phonon scattering by thermal phonons, which takes the $\omega > \omega_c$ phonons below ω_c, will be greater at -5 dB due to the phonons being initially nearer to ω_c.

5.2.3. Low powers at low pressures. At low powers, -20 dB, the number of phonons injected is very low and so the interactions are negligible. The injected phonons with $\omega < \omega_c$ rapidly decay and by 2.3 mm there are only two groups of phonons, those with $\omega > \omega_c$ and the ones with $\omega < 2\Delta_{Al}$. The lack of phonons with $\omega \sim 2\Delta_{Al}$ is indicated by the lack of a sharpening of the leading edge of the signal with temperature, which is seen at -5 and -14 dB; compare figure 11 with figures 9 10. Also at this power and distance the $\omega > \omega_c$ signal is temperature-dependent unlike at higher powers; this is because without any interactions increasing the number of $\omega > \omega_c$ phonons, their number is just attenuated.

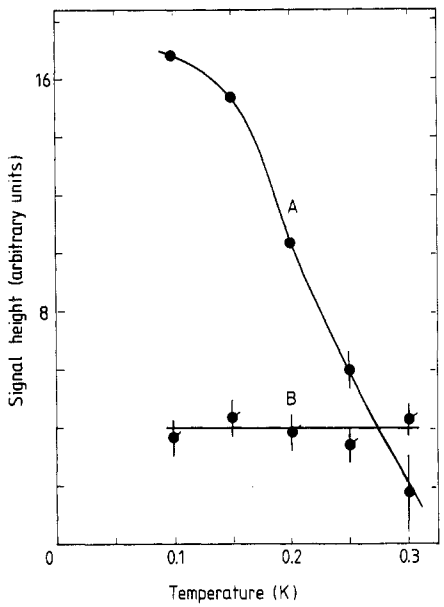

Figure 12. The signal height as a function of ambient temperature for the ω_c signal at 20 dB attenuation (curve A), and the $2\Delta_{Al}$ signal at 14 dB attenuation (curve B). The heater–detector distance is 7 mm and the pressure 6 bar. The lines are guides for the eye.

At 7 mm there are only $\omega > \omega_c$ phonons with no sign of the fast-phonon peak seen at −14 dB. The $\omega > \omega_c$ signal shows a fast decrease with temperature and the attenuation is greater than at higher powers at this distance. This is to be expected as the attenuation occurs over the full distance from heater to detector. This is shown in figure 12.

6. Conclusions

The propagation of phonons with $\omega > 4.5$ K in liquid ^{4}He divides into three groups. At high pressures and all injected powers the propagation is reasonably ballistic because the only scattering is the weak four-phonon process. There is scattering from injected rotons near the heater and this broadens the received signal. The signals are approximately proportional to heater power, they are pressure-independent above 16 bar where the three-phonon process is ineffective and they are independent of temperature below 0.3 K, at least, because the weak four-phonon scattering makes little difference to the phonon spectrum. There is only a small dispersion of the signal, which indicates that most of the detected phonons have $\omega < 10$ K.

The second group consists of low pressures and low powers. This behaviour at low temperatures is dominated by the strong three-phonon process. Pressure has a very strong effect through the pressure dependence of the critical energy for spontaneous decay, ω_c. The decay process can create two or more phonons.

A detailed fit to the data at −20 dB can be obtained using two Planck spectra, one with an effective temperature of 0.9 K from the background channel phonons and the other with a temperature of 1.85 K from the peak channel phonons, which reflects the temperature of the heater.

This phonon group with $\omega > \omega_c(P)$ increases approximately linearly with power but at medium powers it reaches a plateau. It is suggested that the reason for this is four-phonon scattering with the low-energy injected phonons. This is the same process

that causes the temperature dependence when the low-energy phonons are thermally produced. The four-phonon scattering can lower the phonon energies to ω_c and then spontaneous decay reduces the energy to below the detector threshold.

The third group consists of low pressures and high powers. The behaviour is then dominated by phonon interactions within the beam. The dominant process is the reverse of the spontaneous decay process. The interactions cause several effects. Firstly, the spectrum of low-energy phonons is pushed to higher energies and the tail of this spectrum can extend beyond $\omega = 2\Delta_{Al}$. These phonons give a fast signal at the ultrasonic velocity. At medium powers this can be seen together with the $\omega > \omega_c$ phonon signal. As the power is increased, the fast signal grows non-linearly, as would be expected as it arises from interactions.

The strong interactions also increase the number of phonons with $\omega > \omega_c$. Without this effect the $\omega > \omega_c$ signal decreases with ambient temperature, but with high powers and short distances the signal due to $\omega > \omega_c$ phonons does not change with temperature up to 0.3 K. Furthermore the point at which temperature-induced decays of the $\omega > \omega_c$ phonons start can be an appreciable distance in front of the heater. This shortens the effective path length for decay and so these phonons are attenuated less than at lower powers, for the same heater–detector distance.

It is suggested that the increase in $\omega > \omega_c$ phonons is due to the inverse of the spontaneous decay process. This can elevate the energy to ω_c but not higher, but at this energy four-phonon scattering with low-energy phonons can take the energy above ω_c. This process will mostly increase the phonon population just above ω_c, in contrast to injection, which populates over a broader range of energies. The difference in these two spectra will show up in the temperature dependence at large heater–detector distances. The phonons just above ω_c are attenuated more as they have a greater chance of randomly walking over the ω_c edge. This depletion of the $\omega > \omega_c$ phonons just above ω_c can also be seen in the development of the pulse shape with distance, as a preferential loss of the faster $\omega \gtrsim \omega_c$ phonons.

The notion of a region in front of the heater in which the phonons are highly interacting explains a long-standing problem. Measurements on the angular spreading of phonon beams showed a decrease in the spreading with an increase in pressure [11]. The geometric beam width was defined by a 1 mm wide slot positioned about 1 mm in front of the heater. For the angular width of the beam to be greater than geometric there must be spontaneous decays near the slot rather than near the heater. Previously this could not be reconciled with the expected short mean free path [11].

An interacting beam extending about 1 mm from the heater naturally explains the measurements. It also accounts for the increase in angular width with heater power, which increases the interaction distance from the heater and also increases the phonon spectrum at higher phonon energies, where the spontaneous decay angle is greater. This explanation reconciles these measurements with the known low-energy spectrum of the injected phonons.

In conclusion it appears that a coherent, if complex, picture can be drawn for the behaviour of phonons in liquid ^4He over a wide range of powers and pressures at different distances and temperatures. In some regions of the parameter set a quantitative description can be given, but in other regions, especially at high powers and low pressures, only a qualitative description is possible. Here plausible explanations can be offered to account for the diverse behaviour.

Acknowledgments

The experimental work was done in collaboration with Dr N A Lockerbie and Dr R A Sherlock when they and the author were at the University of Nottingham.

References

[1] Khalatnikov I M 1965 *An Introduction to the Theory of Superfluidity* (New York: Benjamin)
[2] Maris H J and Massey W E 1970 *Phys. Rev. Lett.* **25** 220
[3] Jäckle J and Kehr K W 1971 *Phys. Rev. Lett.* **27** 654
[4] Dynes R C and Narayanamurti V 1974 *Phys. Rev. Lett.* **33** 1195
[5] Wyatt A F G, Lockerbie N A and Sherlock R A 1974 *Phys. Rev. Lett.* **33** 1425–8
[6] Brown M and Wyatt A F G to be published
[7] Wyatt A F G, Lockerbie N A and Sherlock R A 1989 *J. Phys.: Condens. Matter* **1** 3507–22
[8] Henshaw D G and Woods A D B 1961 *7th Int. Conf. Low Temperature Physics* (Toronto: University of Toronto Press) p 539
[9] Eisenmenger and Dayem A H 1967 *Phys. Rev. Lett.* **18** 125
[10] Mills N G, Sherlock R A and Wyatt A F G 1974 *Phys. Rev. Lett.* **32** 978–81
[11] Sherlock R A, Mills N G and Wyatt A F G 1975 *J. Phys. C: Solid State Phys.* **8** 2575–90
[12] Sherlock R A, Mills N G and Wyatt A F G 1975 *J. Phys. C: Solid State Phys.* **8** 300–15
[13] Wyatt A F G and Crisp G N 1978 *J. Physique* **39** 244–5
[14] Crisp G N 1980 *PhD Thesis* Nottingham University
[15] Wyatt A F G, Sherlock R A and Allum D R 1982 *J. Phys. C: Solid State Phys.* **15** 1897–915
[16] Hope F R, Baird M J and Wyatt A F G 1984 *Phys. Rev. Lett.* **52** 1528–31
[17] Anderson A C, Connally J I and Wheatley J C 1964 *Phys. Rev. Lett.* **135A** 910
[18] Stirling W G 1983 *75th Jubilee Conf. Liquid Helium 4* (Singapore: World Scientific) pp 109–11
[19] Slukin T J and Bowley R M 1974 *J. Phys. C: Solid State Phys.* **7** 1779–85
[20] Maris H J 1977 *Rev. Mod. Phys.* **49** 341
[21] Northdurft E E and Luszcrynski K 1978 *J. Physique* **39** 252–3
[22] Wyatt A F G 1987 *Japan J. Appl. Phys.* **26** Suppl. 26–3, 7–8
[23] Korczynskyj Y and Wyatt A F G 1978 *J. Physique* **39** 230–1